



AFRL-RX-WP-TP-2011-4420

FUZZY FIBER SENSORS FOR STRUCTURAL COMPOSITE HEALTH MONITORING (PREPRINT)

K. Lafdi, J. Sebastian, N. Schehl, M. Bouchard, M. Boehle, and L. Linge

University of Dayton

DECEMBER 2011

Approved for public release; distribution unlimited.

See additional restrictions described on inside pages

STINFO COPY

**AIR FORCE RESEARCH LABORATORY
MATERIALS AND MANUFACTURING DIRECTORATE
WRIGHT-PATTERSON AIR FORCE BASE, OH 45433-7750
AIR FORCE MATERIEL COMMAND
UNITED STATES AIR FORCE**

REPORT DOCUMENTATION PAGE					<i>Form Approved</i> OMB No. 0704-0188	
The public reporting burden for this collection of information is estimated to average 1 hour per response, including the time for reviewing instructions, searching existing data sources, gathering and maintaining the data needed, and completing and reviewing the collection of information. Send comments regarding this burden estimate or any other aspect of this collection of information, including suggestions for reducing this burden, to Department of Defense, Washington Headquarters Services, Directorate for Information Operations and Reports (0704-0188), 1215 Jefferson Davis Highway, Suite 1204, Arlington, VA 22202-4302. Respondents should be aware that notwithstanding any other provision of law, no person shall be subject to any penalty for failing to comply with a collection of information if it does not display a currently valid OMB control number. PLEASE DO NOT RETURN YOUR FORM TO THE ABOVE ADDRESS.						
1. REPORT DATE (DD-MM-YY) December 2011		2. REPORT TYPE Journal Article Preprint		3. DATES COVERED (From - To) 01 September 2011 – 01 September 2011		
4. TITLE AND SUBTITLE FUZZY FIBER SENSORS FOR STRUCTURAL COMPOSITE HEALTH MONITORING (PREPRINT)				5a. CONTRACT NUMBER FA8650-09-C-5234		
				5b. GRANT NUMBER		
				5c. PROGRAM ELEMENT NUMBER 62102F		
6. AUTHOR(S) K. Lafdi, J. Sebastian, N. Schehl, M. Bouchard, M. Boehle, and L. Linge				5d. PROJECT NUMBER 4349		
				5e. TASK NUMBER 40		
				5f. WORK UNIT NUMBER LP106500		
7. PERFORMING ORGANIZATION NAME(S) AND ADDRESS(ES) University of Dayton 300 College Park Avenue Dayton, OH 45469				8. PERFORMING ORGANIZATION REPORT NUMBER		
9. SPONSORING/MONITORING AGENCY NAME(S) AND ADDRESS(ES) Air Force Research Laboratory Materials and Manufacturing Directorate Wright-Patterson Air Force Base, OH 45433-7750 Air Force Materiel Command United States Air Force				10. SPONSORING/MONITORING AGENCY ACRONYM(S) AFRL/RXLP		
				11. SPONSORING/MONITORING AGENCY REPORT NUMBER(S) AFRL-RX-WP-TP-2011-4420		
12. DISTRIBUTION/AVAILABILITY STATEMENT Approved for public release; distribution unlimited.						
13. SUPPLEMENTARY NOTES PAO Case Number: 88ABW 2011-4784; Clearance Date: 06 Sep 2011. Document contains color. Journal article submitted to <i>Composite Science and Technology</i> .						
14. ABSTRACT Fibers used in composite materials can be coated with carbon nanotubes in a configuration where the nanotubes grow radially away from the fiber surface. In this configuration, the fiber takes on a fuzzy appearance. The network of nanotubes acts as a somewhat conductive coating. This research was a preliminary exploration of fuzzy fiber response to mechanical stimulus, with an eventual goal of incorporation into advanced composite structures, where they would be used to sense strain or crack growth. The resistance change of the fuzzy fibers to applied strain was measured in the following configurations: individual fiber, fiber tow, tow in matrix, and tow in laminated composite. Use as a strain sensor appears promising, where fuzzy fiber tows could be incorporated as a small percentage of a structure. In this arrangement they are non-parasitic, integral, load carrying members of the structure, with the potential to provide wide-area detection of damage.						
15. SUBJECT TERMS carbon nanotubes (CNT), composites, strain measurement, electrical resistance, health monitoring						
16. SECURITY CLASSIFICATION OF:			17. LIMITATION OF ABSTRACT: SAR	18. NUMBER OF PAGES 26	19a. NAME OF RESPONSIBLE PERSON (Monitor) Charles Buynak	
a. REPORT Unclassified	b. ABSTRACT Unclassified	c. THIS PAGE Unclassified			19b. TELEPHONE NUMBER (Include Area Code) N/A	

Fuzzy Fiber Sensors for Structural Composite Health Monitoring

INTRODUCTION

The onset of local damage in structures, such as delamination, cracking and fastener loosening can often be difficult to detect and has long-term implications on the performance of the composite structure. These structures are often exposed to a variety of conditions, including impact, shock loading and extreme changes in temperature. Because of both manufacturing requirements and design specifications, large and complex sections often need to be joined together to form the final structures. It is important to understand the failure behavior of these joints under a variety of static and dynamic loading conditions. Basic understanding of the nature and progression of damage in the structural connections is crucial to the development of optimized joint designs and accurate life prediction strategies.

Non-destructive techniques, such as X-ray or ultrasonic inspection, can shed some light on local damage, but frequently connections may be required to be disassembled for inspection and then reassembled. These techniques are not capable of real-time monitoring of damage evolution. Acoustic emission is often utilized during testing to detect the occurrence of damage connections, but interpretation of the results is often qualitative or the analysis complex. As a result, it is crucial to develop innovative techniques to monitor the state of damage in composite structures.

Structural Health Monitoring (SHM) seeks to provide ongoing monitoring of a structure's integrity, minimizing the need for programmed inspections and allowing maintenance to be need-driven, rather than usage-driven. Current SHM approaches often use strain gages, accelerometers and, more recently, piezoelectric sensors. These provide "point" measurements of engineering information; therefore, they must be placed at or near critical regions of interest in order to detect damage. Should damage occur at other unanticipated regions, it may go undetected. Methods have been devised to use the sensors in a network to "triangulate" readings/locations of interest. This is especially true for piezoelectric sensors, which provide an actuation, as well as a sensing function [1, 2]. One approach to wide-area damage detection is to harness the ability of certain classes of materials to provide a self-diagnosing function. Schulte's group has reported that measuring changes in electrical resistance of carbon fiber reinforced plastic composites during tensile and fatigue loading can be used as an NDE technique [3, 4]. The same idea was used to detect the water leakage in reinforced concrete, in which the cement mortar conductivity decreased with decreasing water content and leakage [5]. The proposed effort seeks to harness the inherent conductivity of carbon nanotubes (CNTs) to provide for in-situ sensing of structural damage [6].

CNTs are made of graphene sheets of hexagonal structure rolled up into a nanoscale tube. For single-walled carbon nanotubes (SWCNTs), only one graphene sheet is used to form the tube. Additional graphene tubes around the core of a SWCNT lead to multi-walled carbon nanotubes (MWCNTs). These CNTs have diameters in a range between one to tens of nanometers, with both their ends normally capped by fullerene-like structures. The unique structure of CNTs brings the material some outstanding properties that make it possible to apply CNTs to applications in

various areas of materials, including the development of a new generation of sensors. Electrochemical sensors and biosensors are among the most intensively studied applications for CNTs. CNTs are a promising material for detecting chemicals and biochemicals due to several intriguing properties, including their outstanding ability to mediate fast electron-transfer kinetics for a wide range of electroactive species and large length-to-diameter aspect ratios that provide high surface area. This large surface area offers an opportunity for depositing external materials or performing surface functionalization that may bring or enhance activity of electrodes [6-9]. Features that make CNTs impressive for electroanalytical applications include the ability to promote electron transfer in electrochemical reactions, high electrocatalytic activities towards chemicals and biomolecular species, and anti-fouling capability of the electrode surfaces [10-13].

The CNT's large surface area gives significant gas-molecular adsorption capacity. The adsorption of electron withdrawing or donating gas molecules on CNTs can cause charge transfer between the nanotubes and molecules [14]. This charge transfer can lead to changes in the electrical conductance of the nanotubes. The direct change in their electrical properties in response to the interaction with probed molecules forms the basis for gas molecular sensors.

Coatings or modification of the nanotubes with certain metals (*e.g.*, Pd nanoparticles [15], etc.), metal oxides (*e.g.*, SnO₂ nanoparticles [16], etc.), polymers (*e.g.*, polyethyleneimine [17] and poly-(*m*-aminobenzene sulfonic acid [18], etc.) have been demonstrated to impart selectivity to the sensors for certain gases and vapors, as well as to allow for detection of molecular species at low concentrations. Functionalization of CNTs may also give biomolecular recognition that may lead to biosensors in addition to the gas and vapor molecular sensors based on change of electrical conduction [19]. In addition to coating or surface modification, doping CNTs with certain elements (*e.g.*, nitrogen doping during CNT synthesis) can enhance sensitivity and selectivity to certain gas molecular species.

Strain and bending of CNTs may cause reproducible changes in their conductance, making it possible to construct electromechanical sensors [20,21]. The piezoresistance properties of CNTs in polymeric composites are being investigated for smart structure applications [22-23]. There are a number of other CNT sensors under study that may have working principles completely or partially different from the above sensors. For example, based on the change of mechanical resonant frequency of CNTs due to variation of temperature, pressure, mass, and strain, the corresponding thermal sensors, pressure sensors, mass sensors, and strain sensors were suggested [24]. Based on the fact that there are shifts of specific peaks in the Raman spectrum of CNTs dispersed in polymeric composites under stress-strain or pressure, CNTs may be used for sensing stress and pressure [25]. In this research study, we will use the unique capability of carbon nanotube based sensors for sensing local composite damage. Through careful design of the specimen it will be possible to detect the onset and progression of damage in the fiber. In the end, the goal of the study is to demonstrate a novel, multi-modal, nanomaterial-based sensor technology that can provide wide-area detection of damage.

MATERIAL FABRICATION

CNT growth on glass fibers (fuzzy glass fiber) was carried out using a traditional chemical vapor deposition process. Two sets of fuzzy glass fiber were prepared by changing only the growth time. CNT fuzzy glass with short resident time exhibits less-dense CNT growth than long resident time (Figures 1 and 2).

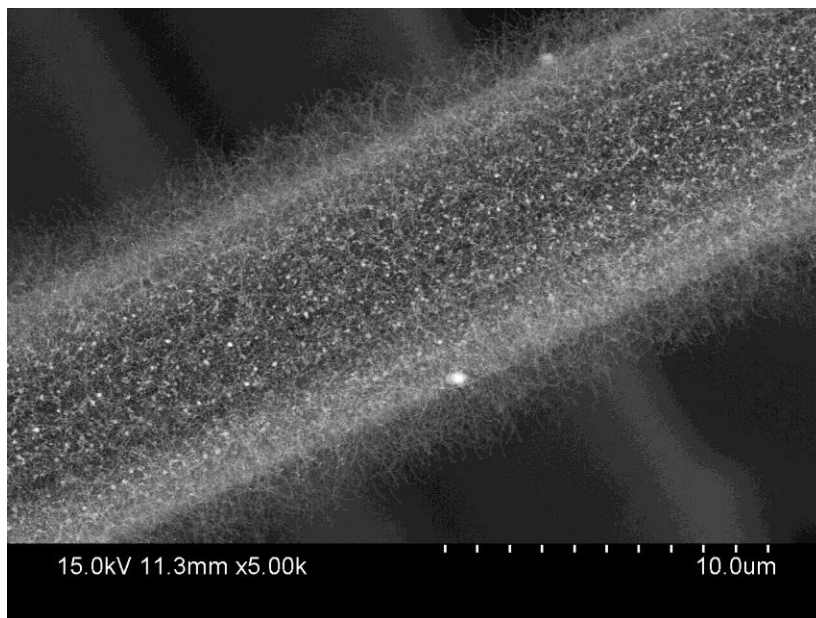


Figure 1. SEM micrograph of low density CNT growth on glass fiber.

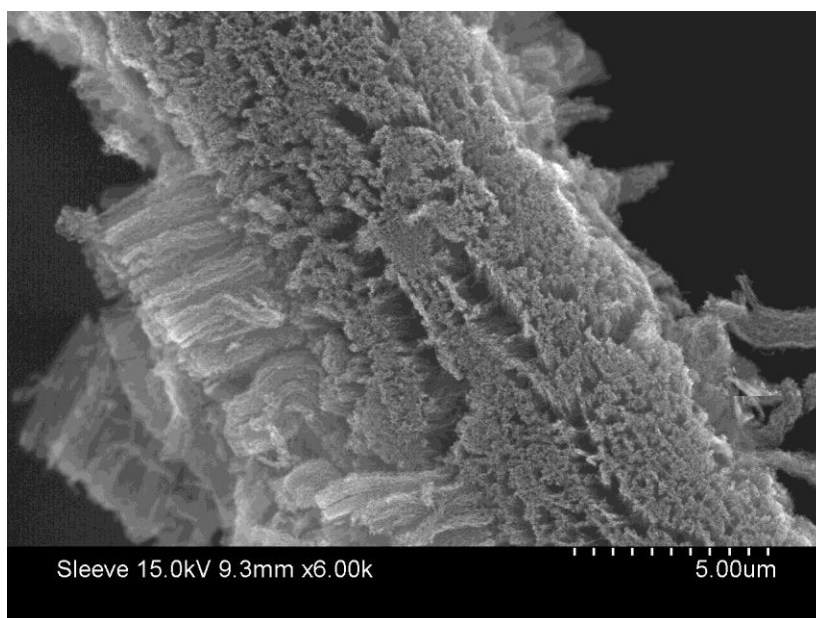


Figure 2. SEM micrograph of high density CNT growth on glass fiber.

SPECIMEN DEVELOPMENT

Fuzzy fiber strain sensors were characterized as fibers, tows, monocomposites (embedded in epoxy matrix material), and composite specimens. Coupon geometries were designed to evaluate specific characteristics of the sensors of interest. Following successful evaluation of individual fibers, single tows were embedded in an epoxy matrix monocomposite and subsequently incorporated into carbon composite specimens designed to produce specific geometry-induced responses. These included straight-sided, stress-concentration, and Poisson's-effect specimens. All composite specimens were fabricated as both unidirectional $[0]_8$ and orthotropic $[\pm 45]_{4s}$ fiber orientations.

Experiments indicated that fuzzy fiber with high density CNTs produced the best strain response, so sensors were developed accordingly for use in the composite specimens. The process of embedding sensors in a carbon composite panel required electrical isolation for the sensor. This isolation was provided by sandwiching the sensor between two layers of plain weave E2 glass having a $0/90^\circ$ fiber orientation. The width of the glass strip was less than 10mm and the length varied with the length of the fuzzy fiber sensor element. Instrumentation leads were bonded to the fiber tow with conductive epoxy and extended beyond the isolation layer.

All composite specimens were fabricated through a similar process. Six composite panels, $12'' \times 12''$, were fabricated with IM7/977-2 prepreg unidirectional carbon fiber tape. Three panels each were prepared with unidirectional $[0]_8$ or orthotropic $[\pm 45]_{4s}$ layups. The three panels of each layup were used for straight-sided, stress-riser and Poisson's effect specimens. Sensors were embedded at specified levels in the layup depending on the type of specimen response to be tested. Panels were then processed in an autoclave. Following cure, specimens were machined from the panels using an abrasive saw. Figure 3 shows a typical cured panel with embedded sensor elements prior to cutting into individual specimen.

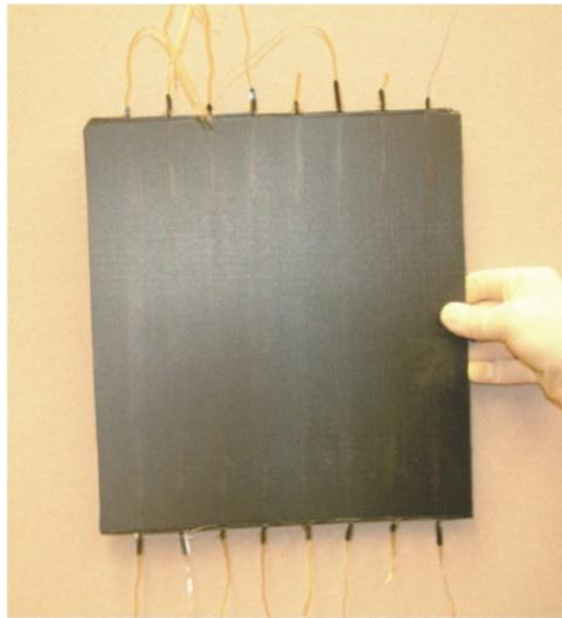


Figure 3. Composite panel with embedded strain sensors oriented for straight-sided specimen.

UNIAXIAL AND ORTHOTROPIC COUPON TENSION SPECIMEN

Two composite panels, one for each layup ($[0]_8$ or $[\pm 45]_{4s}$), were fabricated with 6"-long fuzzy fiber strain sensors embedded at the midpoint of the laminate plies. Eight straight-sided specimens (as shown in Figures 4 and 5), were machined from each panel and tested in a hydraulic test system.



Figure 4. Straight-sided specimen for strain sensitivity measurements.

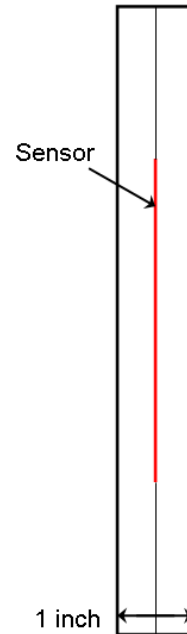


Figure 5. Schematic of straight-sided specimen with embedded sensor depicted in red.

STRESS-RISER TENSION SPECIMEN

Two specimens were designed to further study the fuzzy-fiber sensor behavior in response to stress. An “open-hole specimen” was developed based on ASTM Standard D 5766 “Standard Test Method for Open-Hole Tensile Strength of Polymer Matrix Composite Laminates.” The specimen contained two 3.0"-long sensors to evaluate the response to near-field and far-field stresses around an open hole. In accordance with D 5766 [30], the “width-to-diameter ratio” was maintained through the use of a 3"-wide specimen and a ½"-diameter hole. Two composite layups were fabricated: unidirectional ($[0]_8$) and orthotropic ($[\pm 45]_{4s}$).

Eight fuzzy-fiber sensors were embedded in each layup, two for each specimen, in the longitudinal direction (parallel to the 0 degree unidirectional fibers), as shown in Figure 6. Sensor position was determined by the eventual location of a hole to be machined at the longitudinal midpoint and mid-width of the specimen. Sensors were located at the midpoint of the panels for the unidirectional and orthotropic layups.

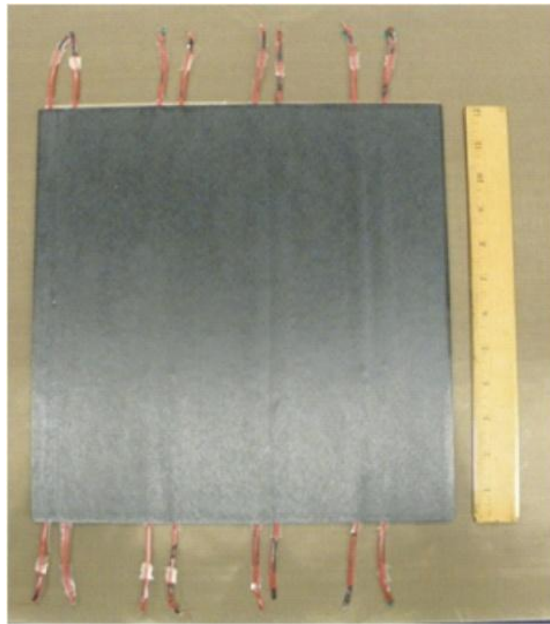


Figure 6. *Fabricated panel with embedded sensors.*

Four specimens were then removed from each panel, cutting parallel to the sensors. A representative specimen is shown in Figure 7 and specimen schematic in Figure 8. Following initial mechanical tests, open holes were machined in the specimens to create the stress concentration.

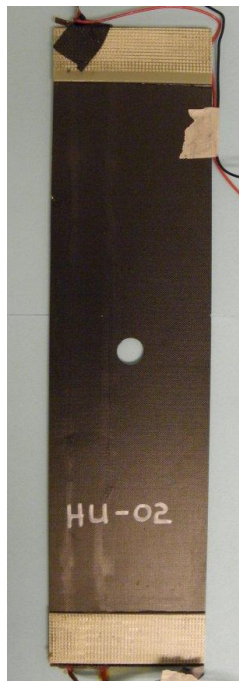


Figure 7. *Open-hole stress-concentration specimen prepared for testing.*

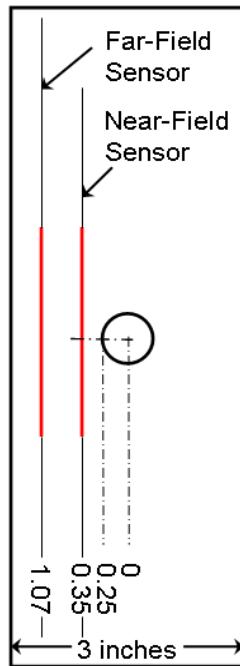


Figure 8. Schematic representative of the sensor locations.

POISSON AND OFF-AXIS TENSION SPECIMEN

Specimens were also designed and fabricated to evaluate sensor response in both longitudinal and transverse orientations relative to the loading axis. The specimens were fabricated in both $[0^\circ]_8$ and orthotropic $[\pm 45]_{4s}$ layups. Two 3.0" long fuzzy fiber sensors were embedded in each layup, one in the longitudinal direction (parallel to the 0° unidirectional fibers) and the second in the transverse direction (perpendicular to the 0° unidirectional fibers). Removal of the specimens from the panel by machining a cut parallel to the longitudinal axis necessitated that all sensor instrumentation wires exit the specimen along its ends rather than sides. Laminates were processed in an autoclave and then machined to a shape that would optimize the transverse sensors response to Poisson effect. Figures 9 and 10 show the specimen in final form and a schematic with sensor locations.



Figure 9. Final form of Poisson's specimen.

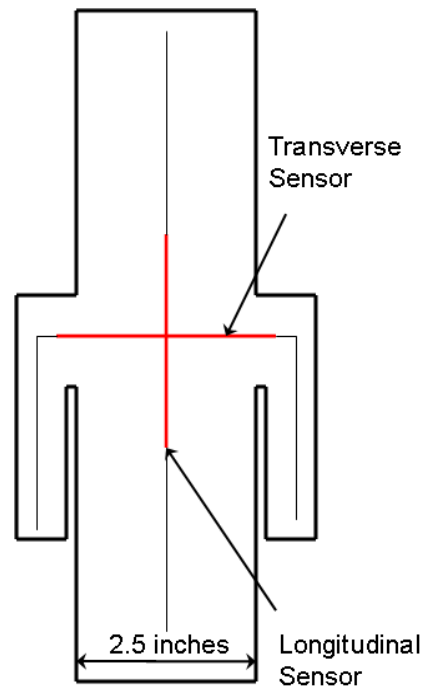


Figure 10. Schematic with sensor locations.

ADDITIONAL OFF-AXIS TENSION SPECIMEN

To further investigate sensor response to longitudinal, transverse, and off-axis loading conditions, a unique specimen was fabricated from randomly-oriented chopped strand fiberglass mat and E-862 Epoxy. The randomly-oriented fiber provided a quasi-isotropic planar specimen which negated any possible influences of fiber directionality on sensor response. The 11-ply specimen contained 4 independent sensors, each at different layers in the laminate. The fabricated and machined specimen is shown in Figure 11. Figure 12 shows the specimen loaded into the hydraulic test machine.

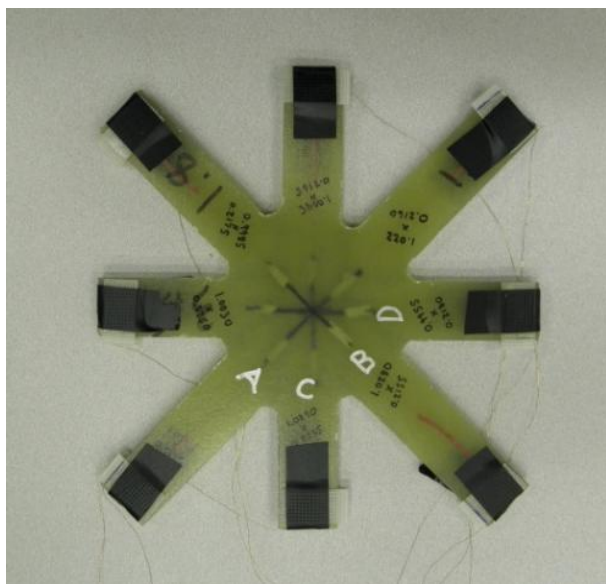


Figure 11. Sensor-orientation specimen machined and ready for testing.

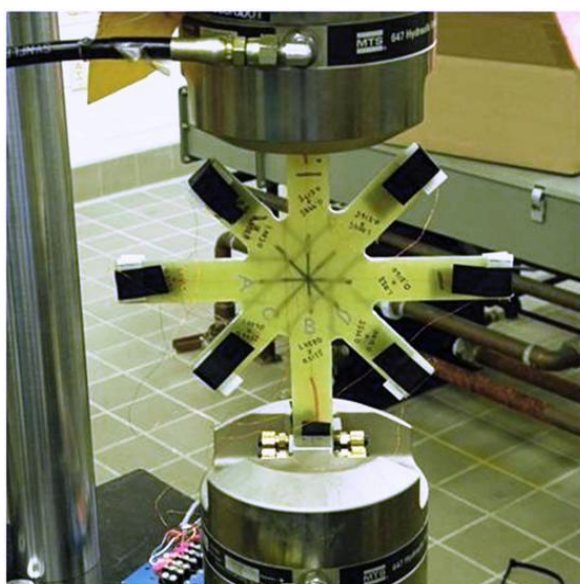


Figure 12. Sensor-orientation specimen loaded into test machine.

INSTRUMENTATION

Two types of signals indicating mechanical strain or damage are available from embedded fuzzy fibers. The first is a loss of continuity, indicating the complete breakage of the fuzzy fiber tow due to an overload or crack propagation. These signals are easy to detect but indicate late-phase damage. It is preferred to detect earlier precursors to such damage, such as an increase in electrical resistance due to applied strain.

In this work, electrical connections were made to the fuzzy fiber sensors with silver-filled conductive epoxy, transitioning to copper lead wires. Since one objective of the fuzzy fiber sensors is to minimally disturb the composition of the structure, it is likely that future implementations would instead transition to wires using CNT-filled matrix material.

The sensors were monitored with a Wheatstone bridge, much the same as a commercial strain gage. The balancing resistor was selected for each fuzzy fiber sensor due to variability in the resistance of the sensors. A Vishay 2310 signal conditioner with a gain of 100 was used to

amplify the sensor response, and bridge excitation was set to 10 V, with no concerns with self-heating due to the large ($>1\text{ k}\Omega$) resistance of the sensors.

UNIAXIAL TENSION TESTING

To get an idea of the piezoresistive behavior of the fuzzy fiber sensor element, initial testing was performed on a tow of fuzzy fibers cast into an epoxy matrix. Specimens were tested in a hydraulic test system as shown in Figure 13, using an MTS 458 analog controller and 100kN servoactuator. Tests were run in load control, at a ramp rate of 10 N/s. Load, strain, actuator stroke, and sensor output were recorded.

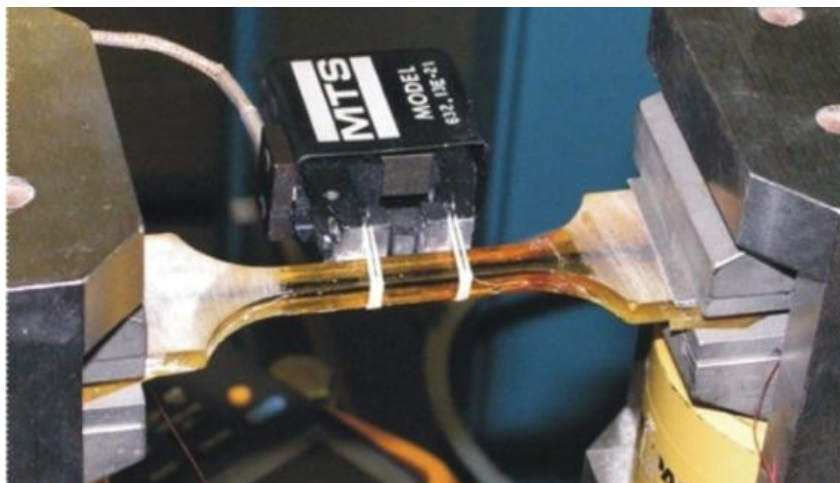


Figure 13. Testing of monocomposite in a hydraulic test system with an extensometer to measure strain.

Tension tests of the straight-sided composite specimens were run next. Tests were run in stress control at ramp rates of 0.2, 2.0, and 20 MPa/s, using a vertical MTS servohydraulic system with a 100kN actuator. Load, strain, stroke, and sensor output were recorded. Tests were stopped at stress levels of 40 MPa for the weaker $[\pm 45]_{4s}$ specimens, and 400 MPa for the stronger $[0]_8$ specimens. An illustration of a typical test is shown in Fig. 14; note that the red lead is clipped to a barely visible sensor wire, not to the extensometer. After inserting the specimen in the load frame and stabilizing the load near zero, these specimens were surrounded by a fiberglass blanket to isolate them from ambient air and allowed to thermally stabilize before testing. Tests at slower rates were repeated if substantial offsets in sensor signal were noted after a test, indicating thermal drift. Sensors in the 13 tested specimens had a nominal resistance in the 50 k Ω range. Additional uniaxial tension tests were performed on the stress-riser specimens. Four specimens of each layup were tested; the sensors in this case had a nominal resistance of 3 k Ω due to differences in processing.

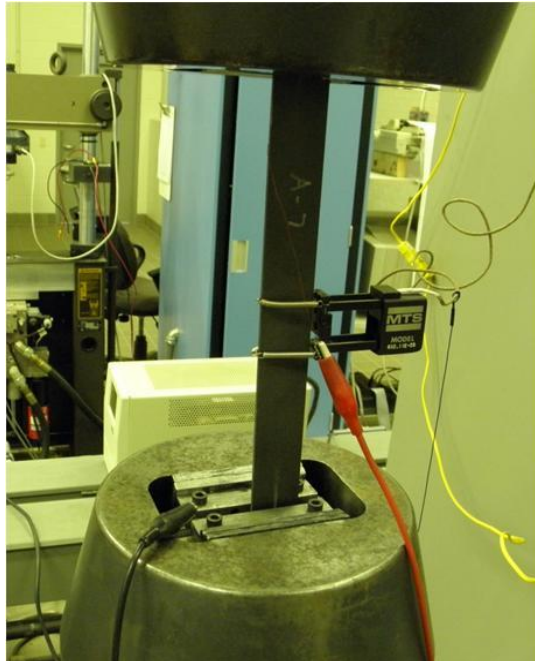


Figure 14. Composite Straight-sided specimen tensile test.

POISSON AND OFF-AXIS TENSION TESTING

Testing of the Poisson's specimen was conducted as shown in Figure 15. The tests were meant to simultaneously evaluate sensor response in both longitudinal and transverse orientations relative to the loading axis, with the same composite layups as in the previous testing. Inclusion of two 75mm long fuzzy fiber sensors, one in the longitudinal direction and the second perpendicular to the loading direction, allowed the evaluation of the response to transverse loading. Test setup was essentially the same as for the earlier tension tests, except for the addition of a second (transverse) channel of sensor amplifier and data collection. The extensometer was moved from the center of the specimen to a section of uniform area. In a second set of tests, the specimens were modified to lengthen the kerf connecting the "body" to the "arms" of the specimen. Sensors in these tests had a nominal resistance in the 50 k Ω range.

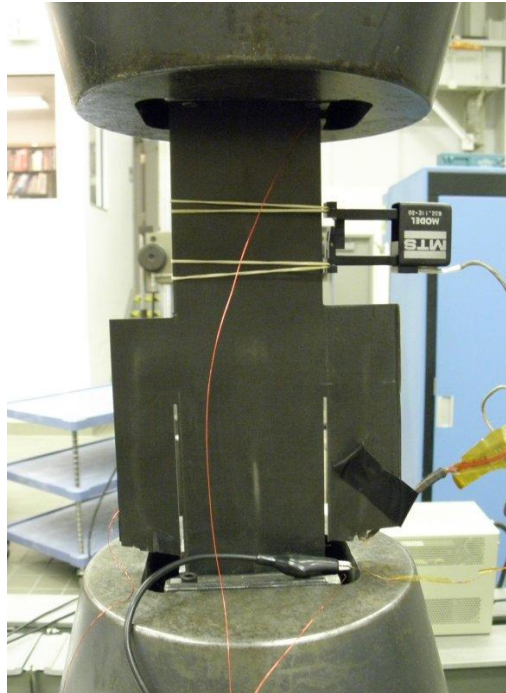


Figure 15. Transverse sensor specimen test setup

The additional off-axis specimen was tested in a different MTS servohydraulic test system with smaller hydraulic wedge grips open on the sides and a digital controller. No reference extensometer was used, but three channels of sensor data were collected at a time. The nominal resistance of these sensors was lower than those used in previous tests, now in the 3 k Ω range. Tests were run dynamically, with a triangle wave of 0 to 1000 lb applied at 0.3 and 0.03 Hz. This load was applied to opposite arms of the specimen, while sensor response was monitored in three of the four possible directions. In order to cancel any effects from sensor location or fabrication, the test sequence was structured so that three channels were connected and, then, the response was recorded to load applied across each of the four sets of arms. One amplifier was moved to the previously unmonitored channel and the test sequence was repeated.

RESULTS AND DISCUSSION

The series of tests noted above progressed from an initial sensor feasibility study to incorporation in segments of actual composite panels. The sensors were shown to produce consistent response, low noise, high strain capability, and were repeatable for elastic strain in same specimen (no hysteresis or offset)

Monocomposite refers to a single tow of fuzzy fibers encased in an epoxy matrix that comprises the majority of the specimen. Several generations of monocomposite were tested before confidence was gained that the tests were representative of the sensor behavior. Figure 16

shows the results from testing two specimens to failure, with extensometer strain used as a reference. These specimens displayed low noise, a consistent response in the elastic region, and reasonable linearity and sensitivity. In addition, they showed the potential for measurement of high strains, well above 1 percent. This was very encouraging and provided enough confidence to move on to the next phase, incorporating the sensors into actual composite panels.

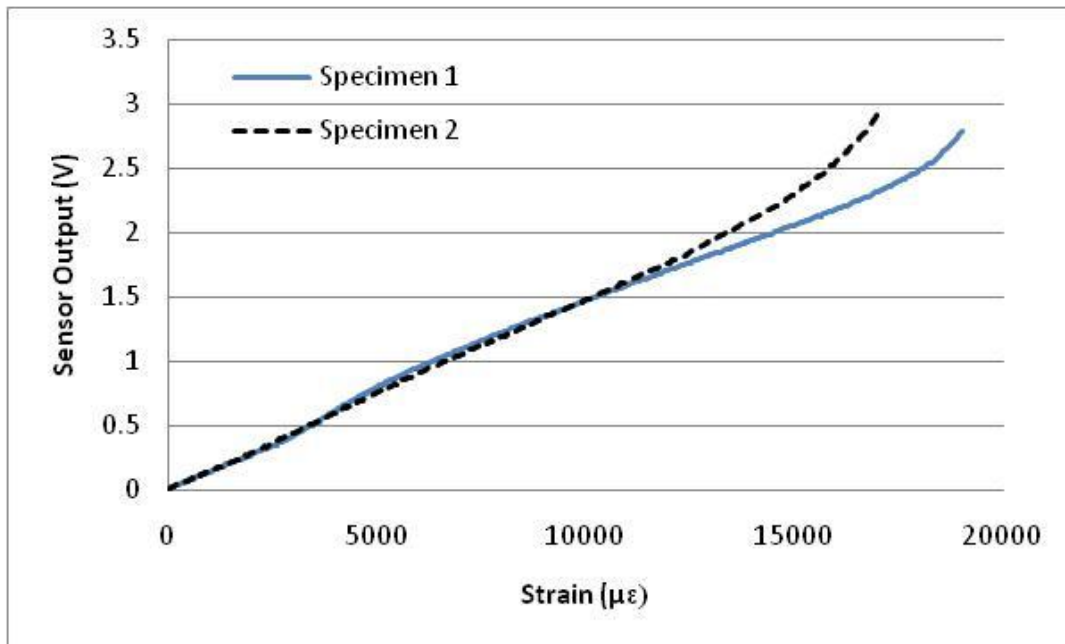


Figure 16. Monocomposite strain test.

Once the test protocol was developed, tension tests showed that sensor response was insensitive to loading rate, but dependent on composite layup. Typical data is shown below in Figures 17 and 18. In both cases, the sensitivity (slope) is almost identical at all loading rates, with slight separation at higher strains. The mean response for 22 tests performed on seven uniaxial specimens was 0.58 mV/με, with a standard deviation of 0.06 mV/με. The mean response for 20 tests performed on six orthotropic specimens was lower (0.41 mV/με), again, with a standard deviation of 0.06 mV/με. The actual data from these tests is shown in Figure 19. If not for the initial outlier, which is unexplained, the orthotropic test standard deviation would have been even lower. Possibly, the additional scatter in the uniaxial data is caused by its higher stiffness or a complex state of stress around the sensor tow; thermal effects (described below) may also play a significant role and might explain the difference in scatter between the two layups. These responses give a mean gage factor for the uniaxial sensor of 2.3 and a gage factor of 1.6 for the orthotropic layup, similar to metal foil gages.

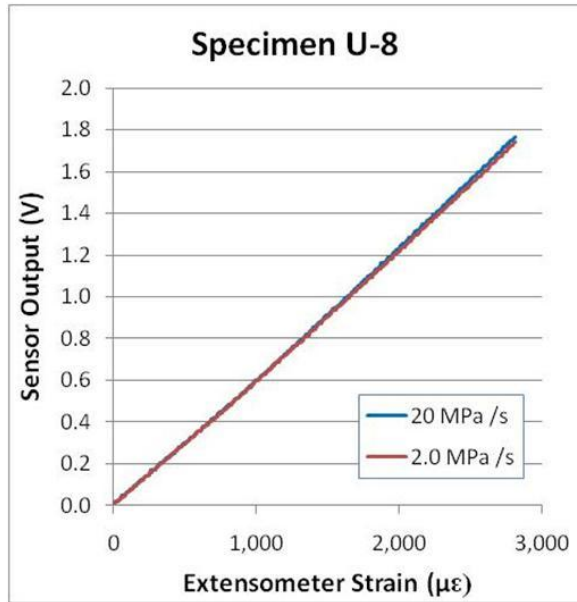


Figure 17. Uniaxial specimen strain data.

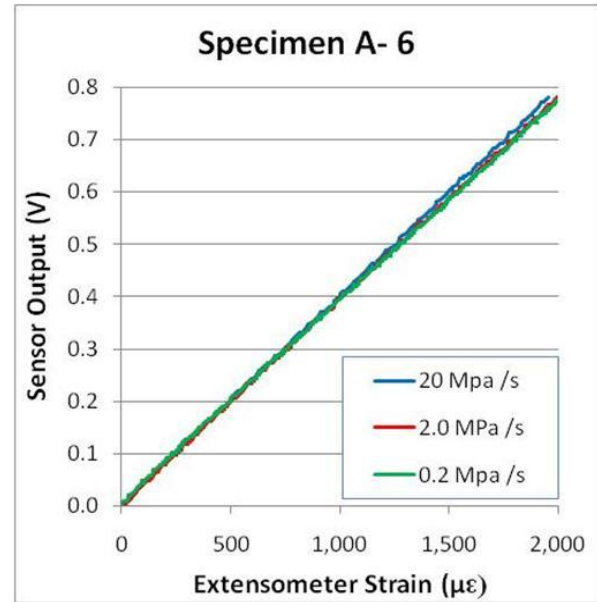


Figure 18. Orthotropic specimen strain data.

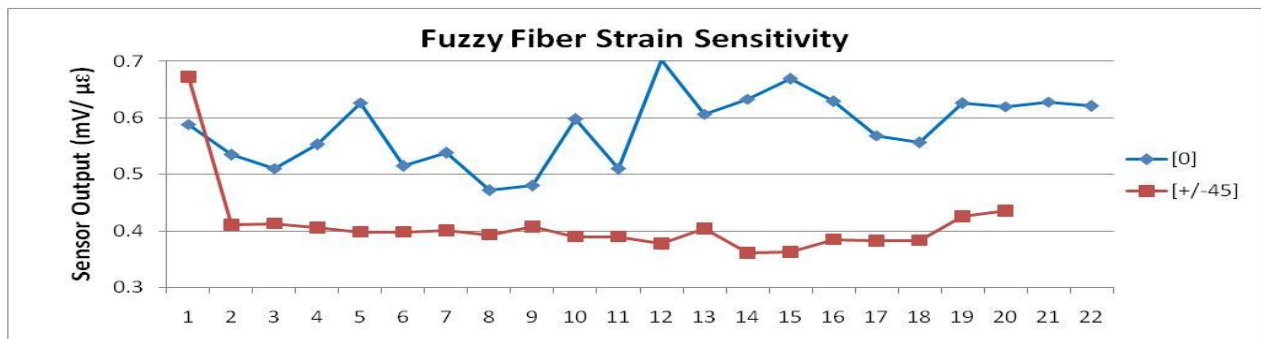


Figure 19. Tension test sensitivity.

The second group of lower resistance ($3\text{ k}\Omega$ as opposed to $50\text{ k}\Omega$) sensors had similar sensitivities, as shown in Figure 20. These specimens were tested twice, with most sensors showing little drift between tests. The first four sensors in Figure 20 are the uniaxial layup and the last four are the orthotropic layup. While the uniaxial sensors have a higher response than the orthotropic sensors, this effect is not as large as in the higher-resistance sensors. A more-pronounced effect is the consistently lower response from S1, the sensor located near the edge of the specimen. This may indicate a different state of stress than seen by the more-central sensor. Again, it appears that the orthotropic layup sensors exhibit lower scatter.

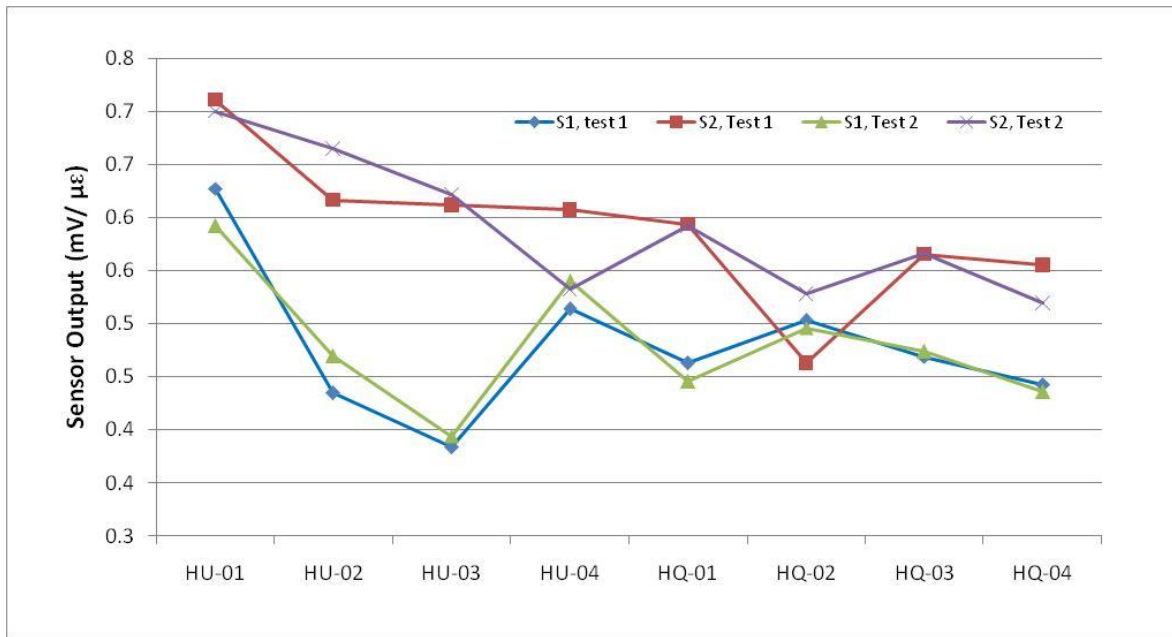


Figure 20. 3 kΩ sensor sensitivity data.

The first off-axis tests involved sensors subjected to transverse loading, with an additional longitudinal sensor as a control. Two specimens of each layup were fabricated and tested. The response of the sensors aligned with the loading direction was, again, consistent with the initial tensile tests, with a uniaxial sensitivity of 0.67 mV/μ ϵ and an orthotropic sensitivity of 0.38 mV/μ ϵ . For the orthotropic layup, the transverse sensor showed a response of -0.13 mV/μ ϵ , an expected value for a Poisson's ratio of ~ 0.3 . However, the uniaxial specimens were not consistent with predictions, as shown in Figure 21. These should have had a much-higher Poisson's ratio and, therefore, stronger lateral contraction. In addition, the transverse sensors showed a positive response, 0.12 mV/μ ϵ . In order to confirm the observed behavior, the specimens were modified to reduce a possible nonuniform stress field at the ends of the transverse sensor, but no substantial change in sensor response was observed. An additional test along the third axis consisted of placing the flat specimen between compression platens and applying a compressive stress; the sensor had zero response to this loading. It is thought that there is a complex interaction between interlaminar stresses and the CNT conduction mechanism. For instance, the compressive load likely had no response because the autoclave cure densified their arrangement, such that additional compression did not cause an increase in conductivity. A related effect may have occurred in the transverse sensors.

In order to further investigate these effects, the additional fiberglass specimen described above was used to look at the longitudinal, transverse, and off-axis response for four sensors simultaneously. In general, these performed similarly to the orthotropic sensors in the graphite-epoxy composites described above. Figure 22 shows the data from one test, where the specimen was loaded along axis "A". The sensor aligned with the loading had the highest response, the sensor at 45° to the loading had a lower positive response, and the sensor at 90° to the loading showed a negative response because of Poisson effects. Due to the lack of a reference strain measurement, the magnitude of these sensitivities cannot be compared directly with results from previous sensors.

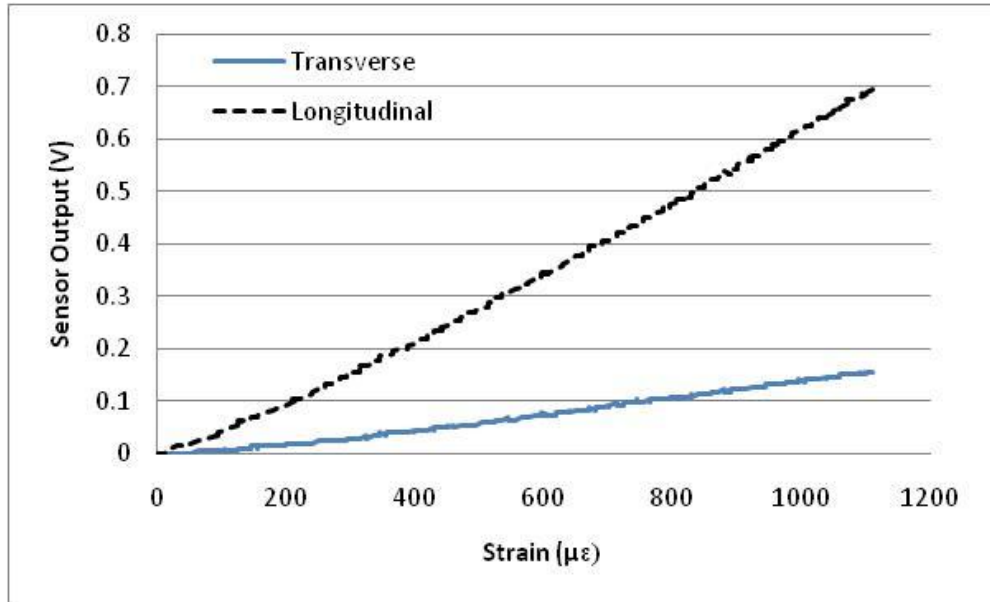


Figure 21. Sensor response in uniaxial composite loaded along its axis.

Figure 23 is a compilation of the sensitivity results from all tests on this specimen, with each data point representing the average of six, twelve, or 24 tests, depending on the sensor and the sensing mode. Data from all sensors was recorded with loading along all axes. In every case, the strongest response was in the longitudinal mode, followed by the oblique mode, and, finally, by the transverse mode, which was negative (or zero for sensor D). Some geometry effect is apparent, as sensors A and B were in the longer arms of the star and C and D were in the shorter arms. The gage length for all four sensors was the same. These tests confirmed the behavior of the fuzzy fiber sensors in an orthotropic composite, but did not provide insight into the anomalous transverse behavior in the uniaxial layup.

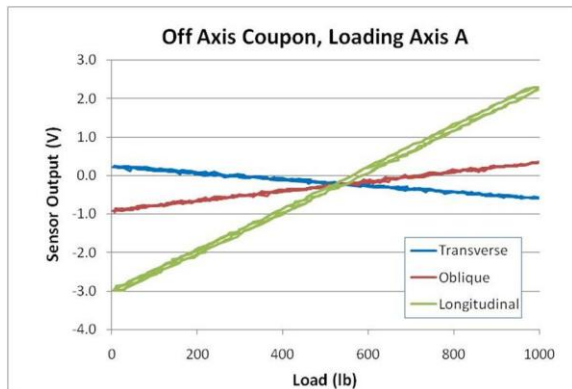


Figure 22. Typical off-axis sensor response.

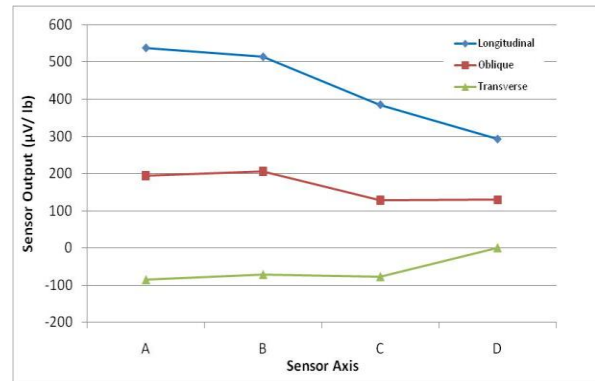


Figure 23. Off-axis sensitivity data.

At the beginning of tensile testing, substantial thermal response was observed, causing unacceptable drift in the strain signal. Faster loading rates or insulating the specimen from the air and allowing it to thermally stabilize before testing overcame the thermal issues. However, a separate investigation was performed to determine the magnitude of error in strain measurement

that could be expected due to thermal errors. For this testing, the specimen was placed in a varied-temperature water bath and the resistance of the sensor was measured across a range of temperatures. The test was performed with one specimen incorporating a first batch ($\sim 50 \text{ k}\Omega$) sensor and one with a second batch ($\sim 3 \text{ k}\Omega$) sensor. Figure 24 shows the thermal response of the sensors. This is a substantial change in resistance, as it corresponds to a potential error on the order of $2000 \mu\epsilon/^\circ\text{C}$. Temperature compensation of deployed sensors is indicated if static strain or changes over time are required to be measured. While not explored in this study, this thermal sensitivity indicates the potential for the use of unstrained fuzzy fiber as a temperature sensor.

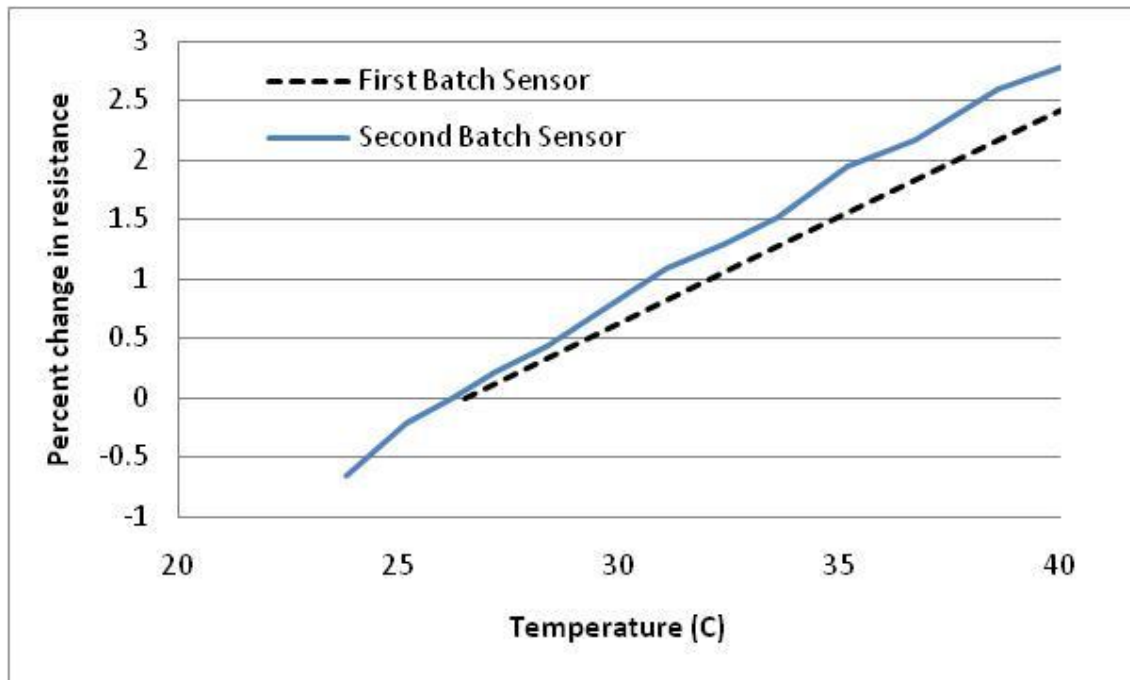


Figure 24. Fuzzy fiber sensor thermal response.

CONCLUSIONS

The efforts presented here highlight the feasibility of incorporating carbon nanomaterials into structural composites as sensors. The CNT covered glass fiber has been shown to be a viable alternative to conventional metal foil strain gages. The fuzzy fiber sensors exhibit similar sensitivity to conventional strain gages and are more easily integrated into composite structures as the sensor itself is a composite. The fuzzy fiber strain gages can be used to sense strain within composite structures and can be readily integrated into the structural laminate to provide sensing over large sections and in locations not accessible to conventional strain gaging techniques.

The unique properties of the CNT covered fuzzy fiber lends itself to application in a wide range of sensing tasks within a structural composite including strain, temperature, degradation, etc. The fuzzy fiber may be tailored so that the same sensor can be used for a multitude of sensing applications. The sensitivity of the fuzzy fiber to a certain stimulus can be amplified by its application so that the sensor will sense the desired parameter, without significant cross talk from other stimuli the sensor may be inherently susceptible to.

Acknowledgments

This research was carried out under Department of Defense contract # FA8650-09-C-5324. The authors are very grateful to Ron Trejo from University of Dayton Research Institute for his support in the processing of composite samples.

REFERENCES

1. D.A. Jones, "Principles and Prevention of Corrosion", Prentice Hall, Upper Saddle River, NJ (1996).
2. X.H. Chen, C.S. Chen, H.N. Xiao, F.Q. Cheng, G. Zhang, and G.J. Yi, *Surface & Coatings Technology*, **191**, 351 (2005).
3. ASTM B117, "Standard Test Method of Salt Spray (Fog) Testing", ASTM International, 100 Barr Harbor Drive, PO Box C700, West Conshohocken, PA, 19428-2959 USA.
4. GM9540P, "Accelerated Corrosion Test", General Motors Engineering Standards, Detroit, MI, USA.
5. Andrews, J., A. Palazotto, M. DeSimio, and S. Olson, "Lamb Wave Propagation in Varying Isothermal Environments", accepted March 2008 for publication in *Structural Health Monitoring* (2008).
6. Olson, S., M. DeSimio, K. Brown, and M. Derriso, "Impact Localization in a Composite Wing Structure," proceedings of the Sensor, Signal and Information Processing workshop, Sedona, Arizona, May 2008.
7. Schulte, *et al*, "Load and Failure Analyses of CFRP Laminates by Means of Electrical Resistivity Measurement", *Composite Sci Technology*, 63; pp. 63-76 (1989).
8. Muto N., *et al.*, "Design of Intelligent Materials with Diagnosing Function for Preventing Fatal Fracture", *Smart Mater. Struct.*, **1**, 1929-1934 (1992).
9. Arai Y., *et al.*, "Measurement of Electrical Conductivity and Detection of Water in Concrete with CFGFRP Used as Electrodes", *J. Ceram. Soc. Japan*, 102(12); pp. 745-51 (1994).
10. M. Pumera, S. Sanchez, I. Ichinose, and J. Tang, "Electrochemical Nanobiosensors", *Sens. Actuators B* 123, pp. 1195-1205 (2007).
11. K. Balasubramanian and M. Burghard, "Biosensors Based on Carbon Nanotubes", *Anal. Bioanal. Chem.* 385, pp. 452-468 (2006).
12. J. Wang, "Carbon-Nanotube Based Electrochemical Biosensors", *Electroanalysis* 17, pp. 7-14 (2005).
13. J.J. Gooding, "Nanostructuring Electrodes with Carbon Nanotubes: A Review on Electrochemistry and Applications for Sensing", *Electrochem. Acta* 50, pp. 3049-3060 (2005)
14. J. Wang, "Carbon-Nanotube Based Electrochemical Biosensors", *Electroanalysis* 17, p. 7 (2005).
15. L. Agui, P., Yanez-Sedeno, and J. M. Pingarron, *Anal. Chim. Acta* 622, p. 11, (2008).
16. M. Pumera, S. Sanchez, I. Ichinose, and J. Tang, *Sens. Actuators B* 123, p. 1195 (2007).
17. K. Balasubramanian and M. Burghard, *Anal. Bioanal. Chem.* 385, p. 452 (2006).
18. M. Trojanowicz, *Trends Anal. Chem.* 25, p. 480 (2006).
19. Y. Sun and H.H. Wang, *Appl. Phys. Lett.* 90, p. 213107 (2007).
20. Y. X. Liang, Y. J. Chen, and T. H. Wang, *Appl. Phys. Lett.* 85, p. 666 (2004).
21. P. Qi, O. Vermesh, M. Grecu, A. Javey, Q. Wang, H. Dai, S. Peng, and K.J. Cho, *Nano Lett.* 3, p. 347 (2003).
22. E. Bekyarova, M. Davis, T. Burch, M. E. Itkis, B. Zhao, S. Sunshine, and R. C. Haddon, *J. Phys. Chem. B* 108, p. 19717 (2004).
23. H.-M. So, K. Won, Y.H. Kim, B.-K. Kim, B.H. Ryu, P.S. Na, H. Kim, and J.-O. Lee, *J. Am. Chem. Soc.* 127, p. 11906 (2005).
24. C. Li, E.T. Thostenson, and T.-W. Chou, *Comp. Sci. Techn.* 68, p. 1227 (2008) .
25. C. Hierold, A. Jungen, C. Stampfer, and T. Helbling, *Sens. Actuators A* 136, p. 51 (2007).
26. E.T. Thostenson and T.-W. Chou, *Adv. Mater.* 18, p. 2837 (2006).

27. A.H. Barber, Q. Zhao, H.D. Wagner, and C.A. Baillie, *Comp. Sci. Techn.* 64, p. 1915 (2004).
28. P. Dharap, Z. Li, S. Nagarajaiah, and E.V. Barrera, *Sensor Review*, 24, p. 271 (2004).
29. C. Li and T.-W. Chou, *J. Intell. Mater. Sys. Struc.* 17, p. 247 (2006).
30. ASTM Standard D 5766/D 5766M, 2002a, "Standard Test Method for Open Hole Tensile Strength of Polymer Matrix Composite Laminate," ASTM International, West Conshohocken, PA, www.astm.org.
31. J.M. Whitney, I.M. Daniel, and R.B. Pipes, "Experimental Mechanics of Fiber Reinforced Composite Materials", Revised Edition, p. 49 (Brookfield Center, CT: Society for Experimental Mechanics, 1984).